



HAL
open science

Optimizing running a race on a curved track

Amandine Aftalion, Pierre Martinon

► **To cite this version:**

Amandine Aftalion, Pierre Martinon. Optimizing running a race on a curved track. 2018. hal-01936993v1

HAL Id: hal-01936993

<https://inria.hal.science/hal-01936993v1>

Preprint submitted on 27 Nov 2018 (v1), last revised 4 Sep 2019 (v2)

HAL is a multi-disciplinary open access archive for the deposit and dissemination of scientific research documents, whether they are published or not. The documents may come from teaching and research institutions in France or abroad, or from public or private research centers.

L'archive ouverte pluridisciplinaire **HAL**, est destinée au dépôt et à la diffusion de documents scientifiques de niveau recherche, publiés ou non, émanant des établissements d'enseignement et de recherche français ou étrangers, des laboratoires publics ou privés.

Optimizing running a race on a curved track

Amandine Aftalion¹ and Pierre Martinon²

¹ Ecole des Hautes Etudes en Sciences Sociales, PSL Research University, CNRS UMR 8557, Centre d'Analyse et de Mathématique Sociales, 54 Boulevard Raspail, Paris, France

² Inria Saclay and CMAP Ecole Polytechnique, Palaiseau, France

E-mail: amandine.aftalion@ehess.fr, pierre.martinon@inria.fr

Abstract. In order to determine the optimal strategy to run a race on a curved track according to the lane number, we introduce a model based on differential equations for the velocity, the propulsive force and the anaerobic energy which takes into account the centrifugal force. This allows us to analyze numerically the different strategies according to the different types of track since the straight line is not always of the same length. In particular, we find that the tracks with shorter straight lines lead to better performances, while the double bend track with the longest straight line leads to the worst performances and the biggest difference between lanes. Then for a race with two runners, we introduce a psychological attraction to follow someone just ahead and the delay to benefit again from this interaction after being overtaken. We provide numerical simulations in different cases. Results are overall consistent with the IAAF rules for lanes drawing, indicating that middle lanes are the best, followed by the exterior lanes, interior lanes being the worst.

Keywords: running strategy, track shape, optimal control, delay problem

AMS classification scheme numbers: 49J15,49N90,92B05,37N25

1. Introduction

It is well known for athletes in races that inner lanes are disadvantageous because of the bent part, while in the outer lanes, there is no one to chase. The aim of this paper is to understand from a physical and mathematical point of view the effect of the curved part of a track and of the lane number on the running performance.

To our knowledge, no optimal control problem including these two effects has been studied. There is a huge literature on the way of running on a curved track, see for instance [6, 14, 23, 25, 28]. Nevertheless, it is never coupled with the psychological effect to have a neighbor on the next lane, which is mentioned as important. Furthermore, though the IAAF regulations do not impose a fixed shape of track, but allow the straight line to vary between $80m$ and $100m$, we are not aware of any study discussing the effect of the straight line length or the shape of the curved track.

In this paper, we will build on a model introduced by Keller [19] and extended by [5, 4], to investigate how the shape of the track and the centrifugal force change the optimal strategy in a race: this leads to longer race times for higher curvatures, and therefore favors the exterior lanes. Estimating the performance of champions based on the modeling of Keller [19] has been developed by various authors [8, 21, 24, 12, 29], but never taking into account so many parameters as in this paper. We will also introduce a model taking into account the psychological effect between two runners. This is made up of two effects: the attraction by a runner close ahead which has a mean effect of decreasing friction on the one hand, and the delay to benefit again from this attraction when overtaken on the other hand. This delay model is inspired by a paper on walking [20]. Let us point out that the mathematical problem encompassing delay in the equations is quite involved. Due to the staggered start positions in the curved part of the track, this rabbit effect is less favorable on the exterior lanes.

After introducing the model, we perform simulations using the optimal control toolbox BOCOP [10]. Since the IAAF regulations do not impose a single shape of track, we analyze the effect of the shape of the track on the optimal velocity profile, as well as the influence of the various parameters of the runner for a single runner. Then we perform simulations for two runners and our results show that the combination of the centrifugal force and the two runners interaction bring a numerical justification to the fact that the central lines are the most favorable to win a race.

2. Race model

2.1. Model for a single runner race

Single runner on a straight track. When a runner is running on a straight line, as used by Keller [19], according to Newton's second law, the acceleration is equal to the sum of forces. We can list two forces, the propulsive force $f(t)$ in the direction of motion, and the friction force, that we assume to be linear in velocity. This leads to the

first equation of motion for the velocity $v(t)$ written by unit of mass:

$$\dot{v}(t) = f(t) - \frac{v(t)}{\tau} \quad (1)$$

where τ is the friction coefficient. This friction coefficient is a rough model which encompasses joints friction, the runner's economy and the elasticity of the track. This friction term could be expanded to take into account more effects such as wind or slopes. Because the runner has a limited capacity, the propulsive force is bounded from above by a constant f_M , that is

$$0 \leq f(t) \leq f_M. \quad (2)$$

Typical values for f_M range from 13 for a sprint at the world level [22] to 5 for a marathon [18].

The power developed by the propulsive force is $f(t) \cdot v(t)$, which is to be taken into account in the energy balance. This energy balance leads to the definition of the oxygen uptake σ introduced in [5], which depends on the anaerobic energy $e(t)$. Note that at the beginning of the race, $e(0) = e^0$, the available energy at initial time, and σ depends on the accumulated oxygen deficit at time t , that is $e^0 - e(t)$. The function σ depends on the length of the race [16]: for short races (up to 400m), σ is a linear increasing function of $e^0 - e$. When the race gets longer, σ reaches its maximal value σ_{max} in the central part of the race, but is increasing at the beginning of the race, and decreasing at the end. Note that σ is the energetic equivalent of $\dot{V}\dot{O}2$, the volume of oxygen used by a unit of time and σ_{max} is related to $\dot{V}\dot{O}2_{max}$. For the shorter races considered in this paper, we assume a linear function σ and note σ_f the final value, thus

$$\sigma(e) = \sigma_f \frac{e^0 - e}{e^0}. \quad (3)$$

This leads to the energy model

$$\dot{e}(t) = \sigma(e(t)) - f(t)v(t), \quad e(t) \geq 0, \quad e(0) = e^0. \quad (4)$$

A champion-level runner has a $\dot{V}\dot{O}2_{max}$ about $75ml/mn/kg$. Since one liter of oxygen produces an energy about $21.1kJ$ via aerobic cellular mechanisms, this provides an estimate of the available energy per kg per second $\sigma_{max} = 75/60 * 21.1 \approx 26$. Furthermore, on a 200m race, $\dot{V}\dot{O}2$ and σ reach only about 75% of their maximal values, so we set $\sigma_f = 20$. We point out that this term is of lower order than \dot{e} .

For a fixed value of the final distance d , the optimal strategy to run the race is obtained by solving the control problem (1)-(2)-(3)-(4) under the constraint:

$$\text{minimize } T, \text{ such that } \int_0^T v(t) dt = d.$$

This problem has been studied in [5, 4, 3]. The parameters are matched to reproduce champions' races. For a race less than 400m, when the function $\sigma(e)$ is decreasing, the velocity is increasing and then decreasing. Indeed, the runner never has enough

energy to maintain his maximal force for the whole duration of the race. Therefore, the optimal strategy is to start at maximal force, and then the force decreases, and so does the velocity.

Since in the optimal control problem, it is usually the distance which is prescribed, in this paper, we choose to take the distance s instead of the time t as variable. We define $y(s)$ to be the time required to run the distance s so that, if $x(t)$ is the distance run in time t , we have

$$\dot{y}(s) = \frac{1}{v(t)} \text{ since } x(y(s)) = s. \quad (5)$$

We call $f(s)$ the propulsive force needed at distance s and $e(s)$ the energy. This allows us to derive the equations for $y(s)$, $f(s)$, $e(s)$, from (1)-(4), which are

$$\ddot{y}(s) = -f(s)\dot{y}^3(s) + \frac{1}{\tau}\dot{y}^2(s), y(0) = 0, \text{ and } \dot{y}(0) = 1/v^0, \quad (6)$$

$$\dot{e}(s) = \sigma(e(s))\dot{y}(s) - f(s), \quad e(s) \geq 0, \text{ and } e(0) = e^0. \quad (7)$$

This formulation requires an initial velocity v^0 which is not zero, but given the effect of the starting blocks where our dynamical model is not correct, assuming an initial velocity of 3 or 4m/s is quite consistent with the effect of the beginning of the race, 10m from departure [26].

The constraint on the force is

$$0 \leq f(s) \leq f_M \quad \text{for } 0 \leq s \leq d. \quad (8)$$

The optimal control problem as such would lead to variations of the force which are too strong. In order to take into account the impossibility for the runner to vary his propulsive force instantaneously, we instead take df/ds as a bounded control. We seek the optimal race strategy to minimize $T = y(d)$.

Centrifugal force on a curved track. For races of 200m or more, the track is not a full straight line, and includes one or several curved parts. While on a curved line, the runner has to move against the centrifugal force, which, by unit of mass, is $f_c = v^2/R$ where v is the velocity of the runner and R the curvature radius. In order to produce a mathematical model for the dynamics in the curved part, we have to take into account the centrifugal force in Newton's law of motion and project this equation on the 3 directions of motion.

Even on the straight line, there is an equation to be written in the z direction: the reaction of the ground, N , is equal to the weight. By the principle of action/reaction, the reaction of the ground is equal to the runner's propulsive force in the z direction. Note that the runner does not have his feet on the ground all the time in the stride: he rather pushes (propulsive force) only for some time in a stride [22]. Some remarks in [2] can be found related to this issue. We point out that there is an interesting explanation of the effect of arms to counterbalance the torque, and that since there are two legs, the reaction on each leg is not exactly the same [6]. In this paper, we will not include these

remarks in the model because we do not think they correspond to the leading effect. The specificity of our work is that although we consider a mean force and mean velocity in a stride, our model allows us to compute an instantaneous force and speed along the race.

On a curve, the runner takes an angle α with the vertical axis to balance the centrifugal force. The runner is subject to gravity g , to the reaction of the ground N along the angle α , and to the centrifugal force $f_c = v^2/R$ (see Figure 1). One has to consider the equations of motion in the centrifugal direction and the z direction, which lead to

$$\frac{v^2}{R} = N \sin \alpha, \quad g = N \cos \alpha \quad (9)$$

which provides the angle according to the velocity and the value of N :

$$\tan \alpha = \frac{v^2}{Rg}, \quad N^2 = g^2 + \frac{v^4}{R^2}. \quad (10)$$

By the principle of action/reaction, the propulsive force in the transverse direction is the opposite of the reaction of the ground in the horizontal direction, hence is equal to $N \sin \alpha$. Moreover, the propulsive force in the vertical direction is $N \cos \alpha$. The total propulsive force F is therefore such that $F^2 = f^2 + N^2$ where we recall that f is in the direction of movement. From (10), we find

$$F^2 = f^2 + N^2 = f^2 + g^2 + \frac{v^4}{R^2}. \quad (11)$$

Since F has to be bounded and g is constant, this leads to the new constraint

$$f^2 + \frac{v^4}{R^2} \leq f_M^2. \quad (12)$$

We point out that eventually the effect of the centrifugal force is taken into account in the force constraint. It cannot have an energy effect directly since the centrifugal force does not produce any work.

Study of the track shape. It is important to know the exact shape of the track since it influences the runner's optimal pacing strategy and performance. However, there is no fixed regulation to build an athletic track. Actually, as indicated in the IAAF manual [1], the length of the straight part can vary between 80 and 100m, while the curved part can be a half circle ('standard' track) or two different circular sections ('double bend' tracks). We choose to study a standard track with an 84.39m straight part, and then two double bend tracks with straight parts of 79.996m and 98.52m respectively. The shapes and dimensions of these tracks are detailed in Figure 2. Note that for races longer than 100m, runners start the race in the curved part. The starting positions are therefore adjusted in order to have the same total distance for all lanes ('staggered start').

Note that each runner is assumed to run at a distance of 30cm from the interior limit of the lane. This is how the radius for the circular parts is set in order to obtain a

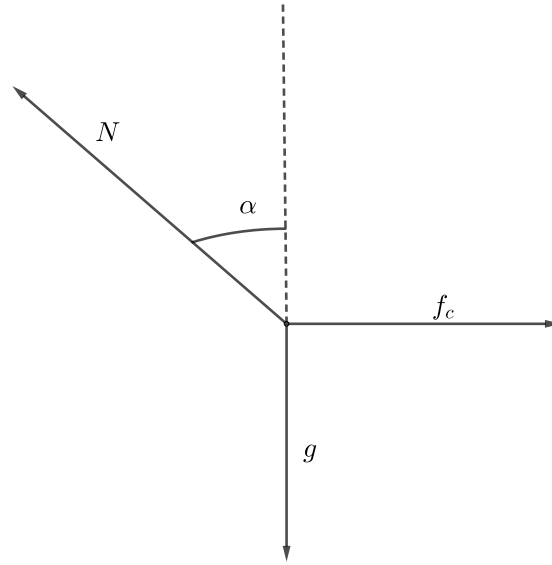
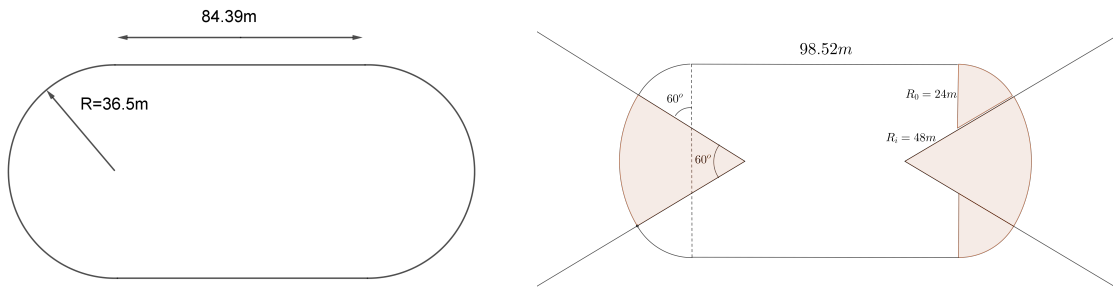


Figure 1. Illustration of the forces on the runner



Track	Straight	Circle	
Standard	84.39m	(36.50m, 180°)	
Track	Straight	Circle 1	Circle 2
Double Bend 1	79.996m	(34.00m, 2 × 70°)	(51.543m, 40°)
Double Bend 2	98.52m	(24.00m, 2 × 60°)	(48.00m, 60°)

Figure 2. Shape and dimensions for standard and double bend tracks.

400m distance for lane 1. Then the width of each lane is 1.22m. This leads to different radii of curvature $R_k(s)$ depending on the lane k and the distance s run on the lane since departure. On the straight part, $1/R_k(s) = 0$. For more details on the value of $R_k(s)$ according to the track, we refer to Appendix A.

We want to point out that at the junction between the circular and straight parts,

the runner will experience a discontinuity in the centrifugal force. This force is 0 on the straight part and can reach a value of the order of $2.5N$ per kilo on the circular part (since $v \sim 10m/s$ and $R \sim 40m$), which is about one quarter of the weight.

We will see on the numerical simulations that this may lead to an acceleration of the runner when reaching the straight part of the track. One could think that it would be better to build a track where the curvature goes smoothly from 0 to the value of the matched circle so that the runner experiences a continuous variation of his centrifugal force. This type of curve, known as a clothoid, is used for instance for railways and roads. The simulations in Section 3 indicate that the final time is actually larger on a clothoid, because the smooth transition leads to a smaller radius for the circular part, therefore a larger centrifugal force.

One of the main results of our simulations is that the tracks with short straight lines lead to better performances (see Figure 6).

Final model for a single runner race. The optimal problem is to minimize $T = y(d)$ with $y(s)$, $f(s)$, $e(s)$ solving (6)-(7), σ being given by (3), with the bounded control

$$\left| \frac{df}{ds} \right| \leq 0.015 \quad (13)$$

and the force constraint coming from (12)

$$f^2(s) + \frac{1}{\dot{y}^4(s)R_k^2(s)} \leq f_M^2 \quad (14)$$

where the curvature radius $R_k(s)$ is prescribed according to the lane k and the track shape, see Appendix A. We use the convention $R_k(s) = +\infty$ on a straight line.

Finally, introducing a state variable for the inverse of speed $z(s) = 1/v(s)$, the optimal control problem for a single runner is

$$(OCP)_1 \left\{ \begin{array}{l} \min y(d), \\ \dot{y}(s) = z(s), \quad s \in [0, d], \quad y(0) = 0, \\ \dot{z}(s) = z^2(s)/\tau - f(s)z^3(s), \quad s \in [0, d], \quad z(0) = \dot{y}(0) = 1/v^0, \\ \dot{e}(s) = \sigma(e(s))z(s) - f(s), \quad s \in [0, d], \quad e(0) = e^0, \\ \dot{f}(s) = u(s), \quad s \in [0, d], \\ |u(s)| \leq 0.015, \quad s \in [0, d], \\ e(s) \geq 0, \quad s \in [0, d], \\ f^2(s) + \frac{1}{z^4(s)R_k^2(s)} \leq f_M^2, \quad s \in [0, d]. \end{array} \right.$$

2.2. Model for a two-runner race

When two runners are involved, we label them with i , $i = 1, 2$ and define $y_i(s)$, $f_i(s)$, $e_i(s)$ respectively the time to reach the distance s , the propulsive force at distance s

and the anaerobic energy left at distance s . We also label by i the parameters of each runner: τ_i the friction coefficient, $f_{M,i}$ the maximal force, e_i^0 the initial energy, v_i^0 the initial velocity. Finally, we call T_i the final time to reach the distance d that is $T_i = y_i(d)$.

Objective function. We want to solve the race problem where both runners try to obtain their minimum time and win the race. The issue is to define a good mathematical problem. Minimizing $\min(T_1, T_2)$ is not enough since it could lead to a situation where one of the runner stops optimizing his race once he knows he will lose. Then, minimizing the sum of the times $T_1 + T_2$ could lead to some cooperative interaction where the faster runner would wait for the slower one to optimize the global time. This is why we choose to minimize a combination of these two objectives, namely minimize

$$\min(T_1, T_2) + k_w(T_1 + T_2)$$

with k_w being a small parameter, for instance $k_w = 10^{-4}$.

We point out that some authors [7, 17] have tried to settle a stochastic description in the framework of game theory but they are not able to handle as many parameters as this model. Also in a short race, we do not believe that there is time to think and adapt one's strategy on the course of the race.

Psychological interaction. When two runners race against each other, we introduce an interaction term which mollifies the friction term of each runner \dot{y}_i^2/τ_i . This term is equal to 1 in case of no interaction, and is lower than 1 in case of a beneficial interaction. It models the psychological benefit that comes from chasing someone just ahead. Note that this interaction is not an aerodynamic effect ('drafting') as in bicycle or car racing, because the velocity is too small. Cognitive effects are known to reduce perceived exertion: a reduction of what there is to put attention on allows runners to be more economical [11, 27]. This psychological effect is indeed acknowledged by runners (sometimes called rabbit effect) and can allegedly have an effect as high as 1 second per 400m lap.

The differential equations for y_1 and y_2 are therefore

$$\ddot{y}_1(s) = -f_1(s)\dot{y}_1^3(s) + \frac{1}{\tau_1}\dot{y}_1^2(s)(1 - F(y_1(s), y_2(s))), \quad (15)$$

$$\ddot{y}_2(s) = -f_2(s)\dot{y}_2^3(s) + \frac{1}{\tau_2}\dot{y}_2^2(s)(1 - F(y_2(s), y_1(s))) \quad (16)$$

where $F(y_1, y_2)$ is to be determined as a function of $r(s)$ which is the distance between the two runners. The detailed expression of $r(s)$ is presented in Appendix A.5.

Basic interaction. We choose the function F of r to be equal to 0.04 when r is roughly between 0 and $-2.5m$. We take the interaction function illustrated in Figure 3

$$F(r) = \gamma H(r + a_1, b_1, \epsilon) H(-r + a_2, b_2, \epsilon)$$

where $\gamma = 0.04$, H a smoothed Heaviside function defined by

$$H(r, k, \epsilon) = (1 + e^{-2k(r+\epsilon)})^{-1} \quad (17)$$

and with the values for the offsets and slopes $a_1 = 2$, $b_1 = 3$, $a_2 = -0.25$, $b_2 = 10$, and $\epsilon = 10^{-6}$.

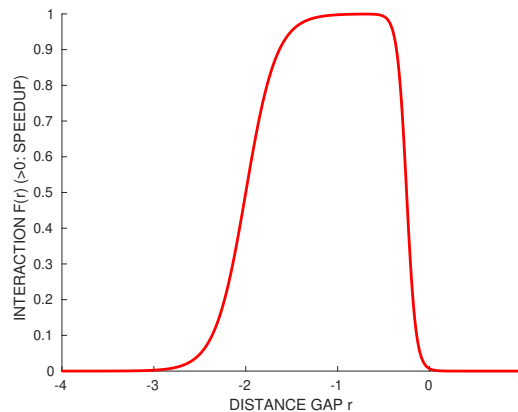


Figure 3. Illustration of the interaction between two runners (for $\gamma = 1$)

Lateral attenuation. It seems reasonable to assume that the positive interaction only occurs when the two runners are close enough to each other. Thus we introduce a limitation of the interaction based on the lane gap between the runners. In practice, the interaction is multiplied by an attenuation function $A(k_1, k_2)$

$$F(r) = \gamma A(k_1, k_2) H(r + a_1, b_1, \epsilon) H(-r + a_2, b_2, \epsilon) \quad (18)$$

with A defined by

$$A(k_1, k_2) = \begin{cases} 0 & \text{if } |k_1 - k_2| \geq 4 \\ 1 - \frac{|k_1 - k_2|}{10} & \text{otherwise.} \end{cases}$$

Inhibition and delay problem.

A refinement of the interaction model is that the benefit should not hold just after being overtaken, since there is a delay in reacting. In order to build a mathematical model for this, we use the behavior of following in pedestrian traffic introduced in [20]. The delay is meaningful in terms of human perception: perception of speed actually comes from successive perceptions of distance over time, and this integration process introduces a delay, while the perception of distances can be considered instantaneous.

We therefore introduce an inhibition formula that suppresses the interaction for a short duration after being overtaken. Since our model is formulated with distance as the independent variable, the delay is also expressed in terms of a distance frame η . The basic idea is to multiply the interaction term F by an characteristic function I_η defined

by

$$I_\eta(s) = \begin{cases} 0 & \text{if an overtaking has occurred on } [s - \eta, s] \\ 1 & \text{otherwise.} \end{cases} \quad (19)$$

For the numerical simulations, I_η is smoothed using the Heaviside approximation H defined by (17). The detection of an overtaking is performed by checking for sign changes of r over $[s - \eta, s]$.

Note that this check relies on **past** values of the state variables used to compute r , thus leading to a **delay** optimal control problem. Delay problems are a quite involved class of optimal control problems, and we refer the interested readers to [13, 9] for recent theory developments. A classical way to solve delay problems is to reformulate them as non-delayed problems, see [15], but the manipulation is rather cumbersome. In our case, we take advantage of the feature from the toolbox BOCOP to handle delays automatically in the fixed final time case (which we have since we use distance instead of time as the independent variable).

Final model for a 2-runner race. We define $T_i = y_i(d)$ and F from (18). The optimal control problem becomes:

$$(OCP)_2 \left\{ \begin{array}{l} \min(\min(T_1, T_2) + k_w(T_1 + T_2)), \\ \dot{y}_i(s) = z_i(s), \quad s \in [0, d], \quad y_i(0) = 0, \quad z(0) = \dot{y}_i(0) = 1/v_i^0, \quad i = 1, 2, \\ \dot{e}_i(s) = \sigma(e_i(s))z_i(s) - f_i(s), \quad s \in [0, d], \quad e_i(0) = e_i^0, \quad i = 1, 2, \\ \dot{f}_i(s) = u_i(s), \quad s \in [0, d], \quad i = 1, 2, \\ \dot{z}_1(s) = -f_1(s)z_1^3(s) + \frac{1}{\tau_1}z_1^2(s)(1 - I_\eta(s)F(r(s))), \quad s \in [0, d], \\ \dot{z}_2(s) = -f_2(s)z_2^3(s) + \frac{1}{\tau_2}z_2^2(s)(1 - I_\eta(s)F(-r(s))), \quad s \in [0, d], \\ e_i(s) \geq 0, \quad s \in [0, d], \quad i = 1, 2, \\ |u_i(s)| \leq 0.015, \quad s \in [0, d], \quad i = 1, 2, \\ f_i^2(s) + \frac{1}{z_i^4(s)R_{k_i}^2(s)} \leq f_{M,i}^2, \quad s \in [0, d], \quad i = 1, 2. \end{array} \right.$$

It is worth pointing out that this optimal control problem has several families of local solutions, typically with a different number of overtakings. In the numerical simulations, we overcome this difficulty by trying several initial points and picking the best solutions. Using a global optimization method would of course solve this problem, however in our case the dimension of the state variables is too high.

3. Numerical simulations for a single runner

In the numerical simulations, we chose to study the 200m race. For reference, in 2018, the world record for 200m is 19.19s (Usain Bolt, Berlin World Championships, 2009). In all the following, we will simulate races with fictitious runners whose parameters (see Table1) are chosen so that their race times are close to 20s.

Runner	τ	e_0	f_M	$1/v^0$	$ df/ds _{max}$
A_1	1.18	1500	9.45	0.43	0.015
A_2	0.85	2160	13	0.43	0.015
A_3	1.7	1000	6.5	0.43	0.015

Table 1. Athletes' parameters

3.1. Single runner on a straight track

We start with a simple straight 200m race to illustrate the effect of parameters f_M , τ , and e^0 . We take as reference athlete A_1 of Table 1. The corresponding speed and force profiles are shown with black lines in Figure 4. The velocity increases to its peak value $v_m \sim f_M \tau$ and then decreases. The runner does not have enough energy to run the whole duration of the race at maximal force. The propulsive force starts at its maximal value f_M , then decreases at the constant rate $|df/ds|_{max}$. The time at which the force begins to decrease depends on the values of f_M and e^0 . Indeed, increasing e^0 does not change the beginning of the race but allows to run longer at $f = f_M$. On the other hand, increasing f_M increases the peak velocity but does not change much the second part of the race. Finally, increasing τ has a more uniform effect and increases the velocity for the whole duration of the race.

3.2. Single runner on a standard curved track

We simulate the same runner on the so-called standard track, i.e. 115.61m half circle of radius 36.80m followed by a 84.39m straight line. Figure 4 shows the race profiles obtained for the interior and exterior lanes (respectively 1 and 8), and the straight line race. The time splits for 50 – 100m, 100 – 150m and 150 – 200m are indicated in the figure: we have chosen the parameters for A_1 so that they match the order of magnitude of time splits for athletes in World Championships. The velocity profiles of the curved track are quite different from the straight line:

i) the runner starts slower because of the curvature: even though he puts his maximal propulsive force at the start, part of it is used to counterbalance the centrifugal force, resulting into a lower effective force and a lower velocity

$$f_M^2 \geq f_{init}^2 + \frac{(v^0)^4}{R_k^2}$$

ii) in the middle part of the race, the maximal propulsive force is reached and we can derive from (1) and (12) the relation between f and v :

$$v = f\tau \text{ and } f_M^2 = f^2 + \frac{f^4 \tau^4}{R_k^2} \quad (20)$$

with R_k the curvature radius on lane k . We can compare this formula with our data: on the straight line $v_s = f_M \tau$, while from (20), the velocity in the middle of the race on lane k is

$$v_s^2 = v_k^2 + \frac{v_k^4 \tau^2}{R_k^2}, \text{ that is } v_k^2 = \frac{-R_k^2 + R_k \sqrt{R_k^2 + 4v_s^2 \tau^2}}{2\tau^2} \quad (21)$$

The numerical simulations indicate an extremely good consistency with this expression: in this case equation (21) yields $v_s = 11.15$, $v_8 = 10.74$, and $v_1 = 10.56$, which are drawn as dashed lines in Figure 4.

iii) after the curved part, there is no more centrifugal force so that the runner can increase both his propulsive force and velocity.

iv) finally, at the end, the runner slows down again, because he does not have enough energy left to sustain his maximal force.

If we compare lane 1 and lane 8, on lane 1 the runner starts slower since the centrifugal force is stronger due to larger curvature. On the other hand, he puts a slightly larger force in the second part of the race, having more energy left, yet he is slower overall. Final times are: 20.43 for the straight line, 20.46 for lane 8, and 20.48 for lane 1.

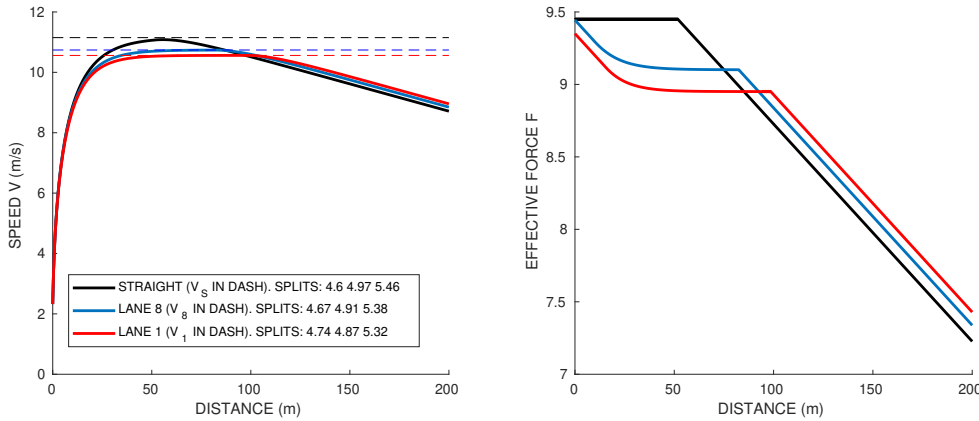


Figure 4. Single runner A_1 on a standard track, lanes 1 and 8, and straight track. Force in N/kg vs distance on the right graph. Speed vs distance on the left graph, with the constant speeds given by eq. (21) in dashed lines. Time splits for 50 – 100m, 100 – 150m and 150 – 200m are indicated.

Now we simulate several runners (see Table 1 for parameters) in order to assess the influence of the maximal force f_M .

Runner with large maximal force f_M . We want to point out that due to the way the curvature is taken into account in the model, see (12), a runner with a greater

maximal force f_M will be less sensitive to the curvature of the track. We illustrate this with the runner A_2 defined in Table 1 whose $f_M = 13$; final times are: 20.31s for straight line, 20.32s for lane 8 and 1. In this extreme case, the runner is basically unaffected by the curvature of the track, that is the curves of velocity and force versus distance are almost the same for straight line, line 1 and 8.

Runner with small maximal force f_M . With a low maximal force $f_M = 6.5$, the runner A_3 of Table 1 can increase his force and velocity when he reaches the straight part of the track, since he has not spent as much energy as the others at the beginning, yet he is slower overall. Final times are: 20.32s for straight line, 20.54s for lane 8, and 20.72s for lane 1.

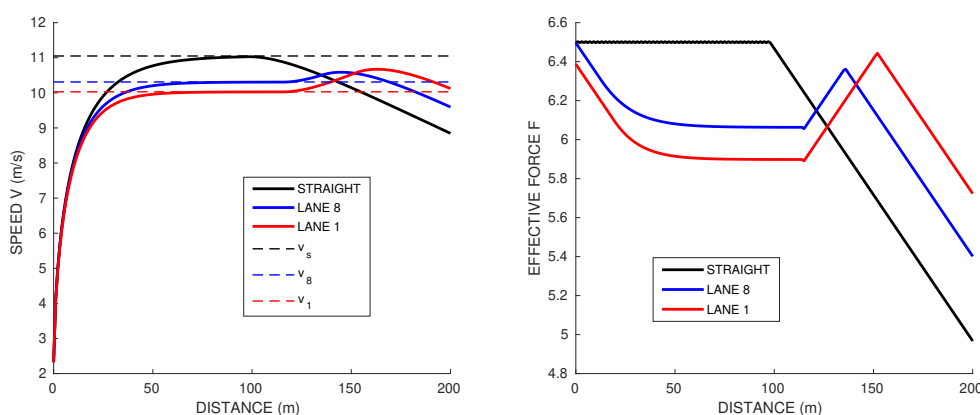


Figure 5. Single runner A_3 on a standard track, lanes 1 and 8, and straight track. Force in N/kg vs distance on the right graph. Speed vs distance on the left graph, with the constant speeds given by eq. (21) in dashed lines. Force and velocity increase when the centrifugal force disappears.

Let us point out that our simulations are consistent with the experiments in [23], where runners are asked to run 60m on a straight part and curved part. The authors observe the existence of two groups, one only mildly affected by the curvature, and the other strongly affected, with as much as 0.2s gap between extreme lanes, which is similar to our gap for runner A_3 .

3.3. Effect of different track shapes

Now we study the effect of different track shapes defined in Figure 2: standard with 84.39m straight (STD), double bend 1 with 80m straight (DB1), double bend 2 with 100m straight (DB2), and two modified standard tracks with smoothed curvature, including clothoid junctions of 10m (CL1) and 30m (CL2). For the clothoid tracks, we choose a straight line of 84.39m as the standard track. As explained in the Appendix, the length of the junctions provides the radius of the circle and the angle, which are respectively 33.32m and 164° for (CL1) and 29.95m and 118° for (CL2). For each track

shape, we simulate the race on the interior and exterior lanes (1 and 8). The results are summarized in Table 2, with the races for runner A_1 (on lane 5) shown in Figure 6. Reference athlete A_1 has a difference of $0.17s$ between the best (DB1 track, lane 8) and worst (DB2, lane 1) case. As mentioned previously, runner A_2 with a very high force $f_M = 13$ is almost unaffected by the curvature, with times varying only between $20.32s$ and $20.36s$. Yet, the DB2 track is still worse than the others. Conversely, athlete A_3 , with a lower force $f_M = 6.5$, is more affected, with $1.01s$ between the best and worst cases. The DB2 is his worst track and his best performance is on the standard track.

Our results show a time difference between interior and exterior lanes ranging from $0.02s$ for the standard track to $0.15s$ for the worst double bend track. This is consistent with [12] who also finds the double bend track to be the worse, using a simplified model based on constant mean velocity and curvature.

Focusing on runner A_1 in Figure 6, we analyze more closely the effect of the track shape and lane:

- DB1 is the quickest track for the exterior lane, though it is very close to STD.
- The standard track has the smallest difference between lanes.
- DB2 is the slowest track, from $0.01s$ on the exterior to $0.14s$ on the interior. When on the outer radius of curvature $24m$, the velocity significantly decreases.
- CL1 is quite close to DB1 and STD, though a little slower. CL2 is slower than DB2 on the exterior lanes, although not as bad in terms of difference between lanes.

It may seem surprising that the tracks with smoothed curvature do not perform better than the ones with a discontinuous curvature. This comes from the fact that the clothoid junction actually results in a smaller radius for the circular part, and thus a greater curvature. The longer the clothoid junction, the more pronounced the effect, and the slower the times.

To conclude, it appears that the track with the shortest straight line is the quickest track for strong athletes in exterior lanes. The standard track shape is the one with the best race times overall, and also the smallest time gap between interior and exterior lanes. On the opposite, the double bend with the long $100m$ straight (DB2) yields the worst times overall, and the highest gap between interior and exterior lanes. These conclusions seem consistent with runners' feelings though there is no study yet of what the ideal shape of track would be for a specific runner.

runner	shape:	STD	DB1	DB2	CL1	CL2	Straight
A_1	lane 1	20.48	20.49	20.62	20.50	20.56	20.43
A_1	lane 8	20.46	20.45	20.47	20.46	20.49	20.43
A_2	lane 1	20.32	20.33	20.36	20.33	20.34	20.31
A_2	lane 8	20.32	20.32	20.32	20.32	20.33	20.31
A_3	lane 1	20.72	20.80	21.55	20.80	21.03	20.32
A_3	lane 8	20.54	20.55	20.66	20.57	20.63	20.32

Table 2. Times for different runners and track shapes.

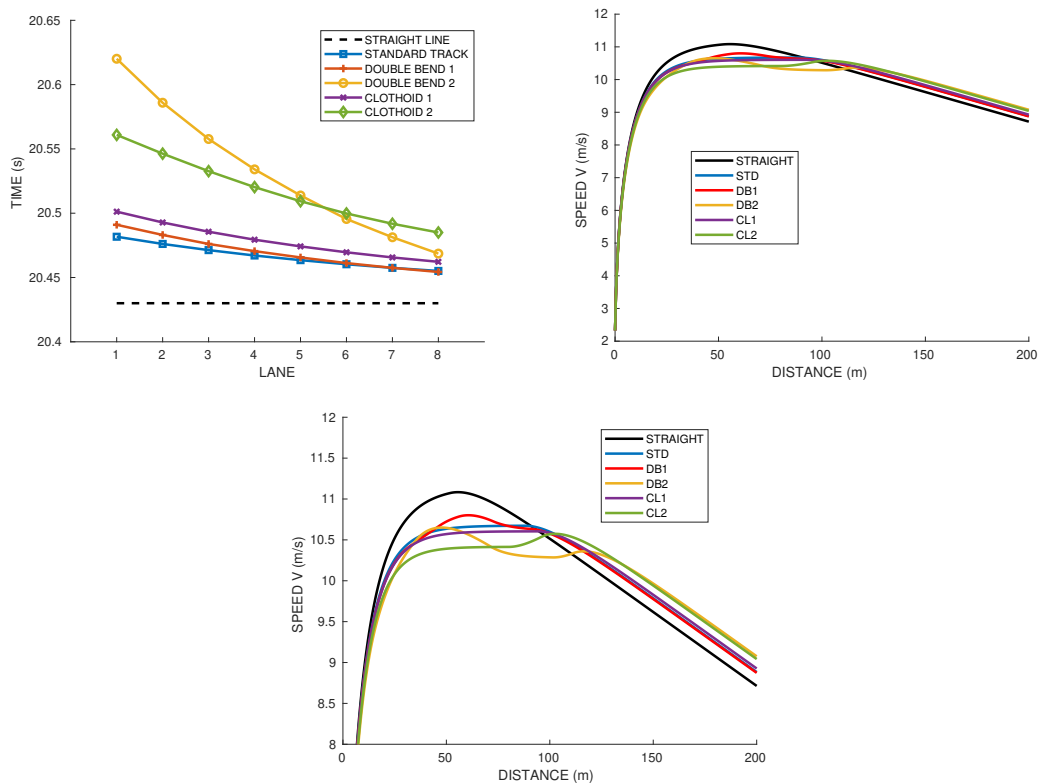


Figure 6. Effect of the track shape on the race time for Runner A_1 vs lane number (left graph). Speed profile for lane 5 (right graph) with zoom. The tracks are standard (STD), double bend 1 (DB1) with short straight line, double bend2 with long straight line (DB2), and curves with short and long clothoid junctions (CL1 and CL2).

3.4. Indoor 200m race

Unlike outdoor 200m races that only cover half the track of a 400m stadium, indoor 200m is run as a full lap on a smaller stadium. The IAAF rules do not impose a fixed track shape and there are strong variations among the different stadiums. In particular the slope of the track can vary. For the stadium shape, we set two straight parts of 45.035m each, connected by two half-circles of radius 17.496m at lane 1, with six 1-meter wide lanes in total. We do not take any slope into account. The results of this race for runner A_1 are shown in Figure 7 (lane 4) and Table 3. On both straight parts the runner increases his propulsive force and velocity. On the curved parts where the total force saturates its limit, we observe once again a good consistency of the speed profile with the constant speed $v_4 = 9.729$ from (21).

The times gaps between lane 1 and 6 are 1.00s, 0.14s and 1.44s for athletes A_1 , A_2 and A_3 respectively. Data from the 2004 World Indoor Championships presented in [28] would suggest a gap of about half to one second, which is rather consistent with the results for our reference runner A_1 . The indoor track favors the exterior lane very strongly.

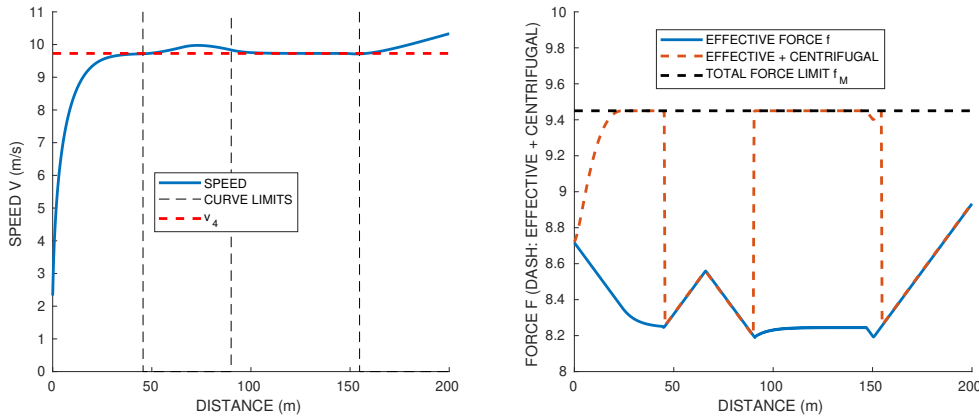


Figure 7. Indoor 200m race (runner A_1 , lane 4). Left figure: speed vs distance. Right figure: forces vs distance. We plot the effective force f and the total force $f + f_c$ with f_c the centrifugal force $f_c = \frac{1}{y^2(s)R(s)}$. On straight parts the centrifugal force is zero.

Runner	lane 1	lane 2	lane 3	lane 4	lane 5	lane 6	1-6 Gap
A_1	21.786	21.542	21.324	21.128	20.950	20.791	0.995
A_2	20.548	20.488	20.454	20.433	20.418	20.407	0.141
A_3	24.116	23.770	23.456	23.171	22.910	22.673	1.443

Table 3. Indoor 200m race. Times for different runners and lanes.

4. Numerical simulations for two runners

We move to the simulations for two-runner races, combining the interaction effect with the curvature effect previously studied for the single runner case. Firstly, we study races with two runners competing in adjacent lanes, to see the effect of the interaction. Then we compute the mean times corresponding to all possible races of a runner versus himself to find that the best lanes are indeed the middle ones.

4.1. Races on different lanes and illustration of the interaction effect

We perform simulations for the optimal control problem (OCP2) for two runners, combining the interaction effect with the centrifugal force. We first set A_1 to be the runner on each lane 1 and 2.

We recall that if A_1 runs alone, his time on lane 1 is 20.485s and on lane 2 20.480s, so of course because of the centrifugal effect, lane 2 is quicker. Due to staggered starts, as soon as we set the interaction, the runner on lane 1 benefits from the interaction at the beginning of the race. First, we set the interaction term $\gamma = 0.04$ but $\eta = 0$. The results are illustrated in Figure 8, with the velocity profile in lane 1 on the left and the interaction for each runner and relative distance on the right. When the relative distance is negative, the runner in lane 1 is behind. So in this case, the runner in lane 2 wins the race and they overtake each other twice: lane 1 starts behind because of the

staggered starts, benefits from interaction and overtakes at $50m$; then lane 2 benefits from interaction right away and is able to overtake again at $150m$. Then they are on the straight line, very close to each other, lane 1 benefits from interaction and is ready to overtake again but loses in the end by $0.04s$.

Then in Figure 9, the interaction term is set at $\gamma = 0.04$, and the inhibition frame is $\eta = 20m$. This means that the positive interaction is disabled when a runner is overtaken in the previous $20m$ of race. Figure 9 shows the speed profile (left graph) and interaction / inhibition terms (right graph). Compared to the race without inhibition in Figure 10, we observe a different behaviour with only one overtaking and the runner on the interior winning by $0.27s$. Note that since we optimize the whole race, there is no reason for the race with inhibition to coincide with the race without inhibition, even before any overtaking occurs. We observe that the inhibition (on the right graph) correctly detects the overtaking and suppresses the interaction accordingly. This prevents the overtaken runner at lane 2 to keep up (and eventually catch up) with the one at lane 1, as we see that the distance gap increases after the overtaking. In the race without inhibition, the overtaken runner was benefiting from the interaction right away, which allowed him to catch up and take the lead back. With inhibition, the runner on lane 1 manages to win the race, though he is on a disadvantageous lane. In the full race, of course, the runner in lane 2 has a neighbour on the other side which changes the total result.

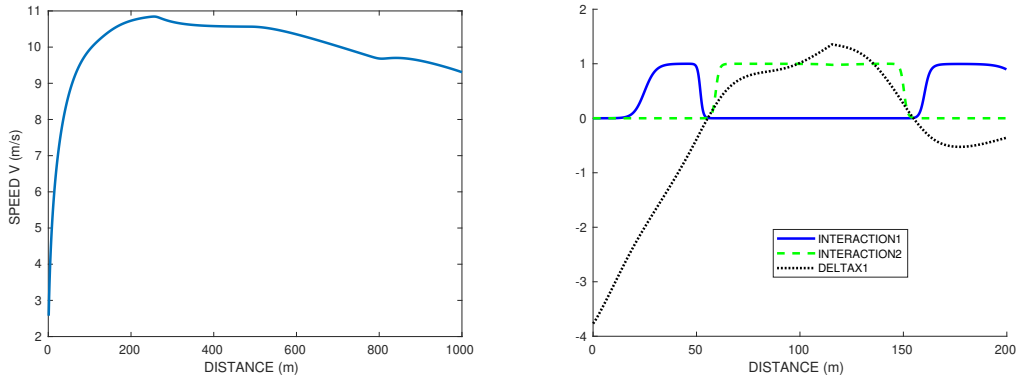


Figure 8. Race A_1 vs himself at lanes 1-2, with interaction $\gamma = 0.04$ and a frame $\eta = 0$ that is no inhibition. Left graph: speed profile and time splits of the runner at lane 1. Right graph: distance gap and interaction term for both runners. The sign change of the distance gap corresponds to the overtaking. Lane 2 wins by $0.04s$.

There are cases where, though the inhibition $\eta = 20$, there are still two overtakings. We study for instance the 5-4 race, with the speed and force profile of the runner at lane 5 shown in Figure 10. Without interaction ($\gamma = 0$), lane 5 wins without any overtakings, with final time $22.47s$. With interaction ($\gamma = 0.04$ and $\eta = 20$), lane 5 still wins after 2 overtakings, with final time $22.23s$. At the start, the runner on lane 4 benefits from the interaction due to the runner at lane 5 being ahead (staggered start). He catches up then overtakes the exterior runner, who in turn gains the interaction, catches up and

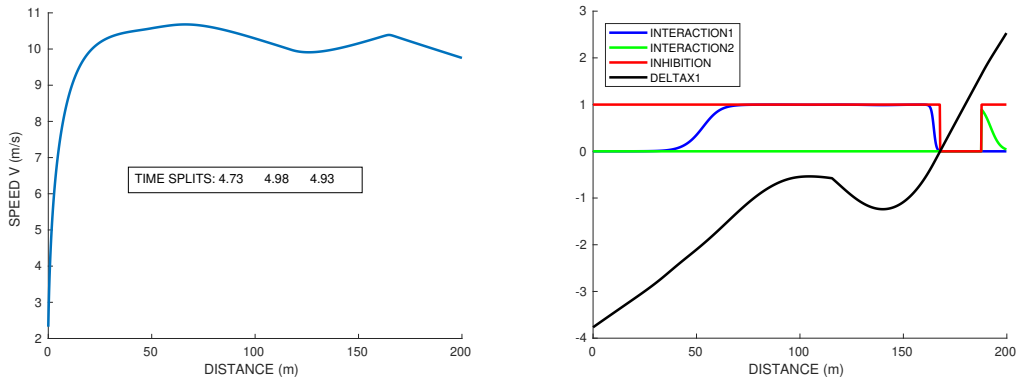


Figure 9. Race A_1 vs himself at lanes 1-2, with interaction $\gamma = 0.04$ and a frame $\eta = 20m$ for the inhibition. Left graph: speed profile and time splits of the runner at lane 1. Right graph: distance gap and interaction term for both runners. The sign change of the distance gap corresponds to the overtaking. Lane 1 wins by 0.27s.

overtakes the interior runner again. At the end the interior runner, being behind, has the interaction again and is catching up with the exterior runner, but too late.

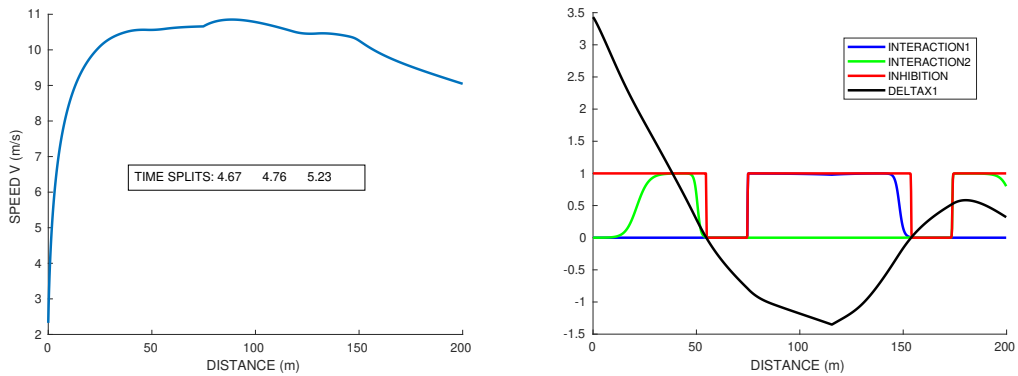


Figure 10. Race A_1 vs himself at lanes 5-4, with interaction $\gamma = 0.04$ and inhibition $\eta = 20m$. Left graph: speed profile and time splits of the runner at lane 5. Right graph: distance gap and interaction term for both runners. The sign changes of the distance gap correspond to the 2 overtakings.

We have also made simulations with runner A_1 vs runner A_2 , and though runner A_2 is stronger in force, on some lanes, runner A_1 can benefit from interaction to be able to win.

We point out that the interaction parameters can be runner dependent since some may be very sensitive to this effect and others much less.

4.2. Mean time per lane

In a real race, there are eight runners, however our model is only for two. Therefore, we simulate a set of races with two identical runners, the first on a fixed lane, the second on each possible other lane. We define $T_1^{k_1, k_2}$ to be the time for the winner in the race between two identical runners A_1 in lanes k_1 and k_2 . We want to compute the average performance at lane i as the mean time

$$\bar{T}_i = \frac{1}{7} \sum_{j=1..7, j \neq i} T_1^{k_1=i, k_2=j}.$$

First, we compute the times $T_1^{i,j}$: the best times in j for each i are indicated in Table 4. In Figure 11, we have plotted the times for $i = 1, 5,$ and 8 . The best times are obtained for the maximal interaction, namely with the second runner on an adjacent lane. For runner A_1 on lane 5, his best performance is obtained with a neighbor on lane 4 rather than 6. We recall that the model includes a lateral attenuation for the interaction, which is 0 when runners are more than 3 lanes apart. If we compare the best time for each case, it is decreasing with the lane.

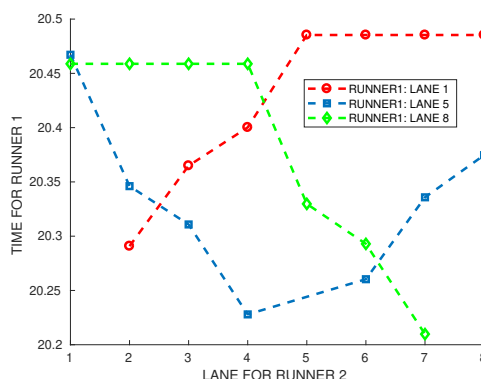


Figure 11. Times for athlete A_1 at lanes 1,5,8, running against himself.

lane	2	3	4	5	6	7	8
solo time	20.480	20.475	20.471	20.467	20.464	20.461	20.459
2-runner time	20.300	20.292	20.283	20.276	20.270	20.264	20.259
time gain	0.180	0.183	0.1880	0.191	0.194	0.197	0.200

Table 4. Athlete A_1 at lane k running against himself at lane $k - 1$. Interaction $\gamma = 0.04$ with inhibition $\eta = 20m$. Race time and gain with respect to solo race time.

We show in Figure 12 the mean times \bar{T}_i obtained for runner A_1 against himself, with an interaction weight $\gamma = 0.04$ and $\eta = 20$ when he runs on each lane i . If we look at the overall performance then lane 5 is the best, followed by lane 6, 4, 7, 3, 8, 2 and

lane 1 is by far the worst. We compare with the solo case ($\gamma = 0$) where of course the exterior lane is the quickest.

The results are nicely consistent with the IAAF drawing rules. Indeed, according to the IAAF rules [1], starting lanes are drawn in three lots:

- a first draw is made for the four best runners in the middle lanes 3,4,5 and 6.
- a second draw is made for the next two runners between the exterior lanes 7 and 8.
- a last draw is made between the runners with the lowest performance to get the interior lanes 1 and 2.

Nervertheless, we find that the interior lanes 1,2 are a real disadvantage, the more so as if the runners are not as strong.

In [25] the authors recall some average time data for Olympics 1996 and 2000, and World Championship 2001: they indicate an average time gap of 0.16s between interior lanes 1 and 2 and exterior lanes 7 and 8. We obtain a smaller gap of 0.047s, which may be due to the fact that we consider identical runners in our simulations, while in actual races the athletes in the exterior lanes were supposedly stronger than those in the interior lanes.

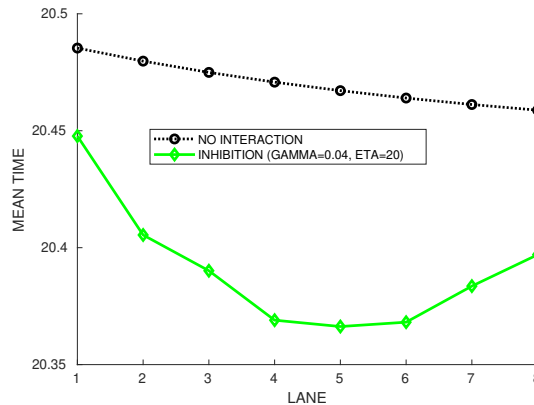


Figure 12. Mean times per lane for runner A_1 when in lane i vs himself in all other lanes. Without interaction ($\gamma = 0$), and with interaction $\gamma = 0.04$, $\eta = 20$. Lane performance (sorted by mean time): $\bar{T}_5 < \bar{T}_6 < \bar{T}_4 < \bar{T}_7 < \bar{T}_3 < \bar{T}_8 < \bar{T}_2 < \bar{T}_1$. Gap $\bar{T}_1 - \bar{T}_8 = 0.050859$.

5. Conclusion

In this paper, we have studied how the geometry of the track and the psychological interaction between runners affect performances. We have introduced an optimal control model taking into account the centrifugal force as a limiting factor for the maximal propulsive force. We couple this with a new model describing the positive interaction exerted by a runner close ahead and the delay to benefit from it after being overtaken. We carry out numerical simulations for several runner profiles on different track shapes. The results indicate that the track with the shortest straight line is the quickest for

strong athletes in exterior lanes. The so-called standard track (straight line and half circle) yields the best performances overall. The double bend tracks with longer straight lines (DB2) are significantly slower. In particular running on lane 1 on the DB2 track appears to be an overwhelming disadvantage.

Furthermore, the combination of the centrifugal and interaction effects leads to the middle lanes being the most favorable, followed by the exterior lanes, with the interior lanes being the worst. These results fit very well with the drawing rules of the IAAF for starting positions, which follow this preference order.

Acknowledgments

The authors would like to thank Cecile Appert and Henk Hillhorst for introducing the delay problem for the inhibition of runners interaction. They also acknowledge enlightening discussions on the topic with Thorsten Emig, Christine Hanon, Jean-Pierre Nadal and Guillaume Rao. They are very grateful to Aurelien Alvarez for providing details on clothoids.

Appendix A. Track shape details

Note that each runner is assumed to run at a distance of 30cm from the interior limit of the lane. This is how the radius of the circular parts is set in order to obtain a 400m distance on lane 1.

Appendix A.1. Standard track

The standard track is made up of a circular half-circle of length $l_c = 115.61\text{m}$ followed by a straight line of 84.39m , for a total distance of 200m , which yields

$$R_1 = l_c/\pi = 36.80.$$

Since the runner is assumed to be 30cm away from the boundary of the lane, the radius of construction is $R_1 - 0.3$.

We denote by R_k the radius for the runner on lane k . Since the width of a lane is 1.22m , the radius at lane k is

$$R_k = R_1 + 1.22(k - 1).$$

Therefore, on a standard track, the radius is given by the expression

$$R_k(s) = R_k \quad \forall s \in [0, l_c], \quad R_k(s) = +\infty \quad \forall s \geq l_c.$$

We denote by $\theta_k(s) \in [0, \pi]$ the angular position of the runner on the curved part on lane k , with convention $\theta_k(s) = \pi$ on the straight part. The staggered start design ensures all lanes have the same total distance. This yields the starting angle

$$\theta_k^0 = \frac{1.22(k - 1)\pi}{R_k}.$$

This goes from 0 for lane 1 to 0.6rad for lane 8. On the curved part, the angular position of the runner on lane k varies in $[\theta_k^0, \pi]$ according to

$$\theta_k(s) = \theta_k^0 + \frac{s}{R_k}.$$

Appendix A.2. Indoor track

The indoor track has a shape similar to the standard track, but is only 200m for a full lap, instead of 400m . We choose a track with two straight parts which have a length of $l_s = 45.035\text{m}$ each. This yields a circle radius at lane 1 of $R_1 = 17.496$. Lanes are smaller with a width of 1m , therefore $R_k = R_1 + (k - 1)$. Compared to the standard track, the staggered start has to compensate for the two circular parts, thus the starting angle is

$$\theta_k^0 = \frac{2(k - 1)\pi}{R_k}.$$

We extend the definition of the angle θ to the interval $[\pi, 2\pi]$ on the second circular part, and 2π on the second straight part.

Another difference is that the limits for the curved parts now depend on the lane. We denote by S_1, S_2 the straight parts and C_1, C_2 the circular parts; the first curved part ends at $l_k := R_k(\pi - \theta_k^0)$. Finally, the angular position for the indoor track is

$$\begin{cases} \theta_k(s) = \theta_k^0 + s/R_k, & s \in C_1 = [\theta_k^0, l_k], \\ \theta_k(s) = \pi, & s \in S_1 = [l_k, l_k + l_s], \\ \theta_k(s) = \pi + (s - l_k - l_s)/R_k, & s \in C_2 = [l_k + l_s, 200 - l_s], \\ \theta_k(s) = 2\pi, & s \in S_2 = [200 - l_s, 200]. \end{cases}$$

Appendix A.3. Double bend track

As for the standard track, let us denote by l_c the length of the curved part, and k the lane number. Let R_o and ϕ_o be the radius and angular width of the outer (smaller) circles, and similarly R_i, ϕ_i for the inner circle. Going from the starting position, we denote by C_1 the first circular part ('outer circle'), C_2 the second one ('inner circle'), C_3 the second 'outer circle', and S the straight part. With $\mu_k = 1.22(k - 1)$ the radius adjustment for each lane, the abscissa limits for C_1 and C_2 are

$$s_1 = l_c - (R_o + \mu_k)\phi_o - (R_i + \mu_k)\phi_i, \quad s_2 = l_c - (R_o + \mu_k)\phi_o.$$

Finally we have the radius expression

$$\begin{cases} R_k(s) = R_o + \mu_k, & s \in C_1 = [0, s_1], \\ R_k(s) = R_i + \mu_k, & s \in C_2 = [s_1, s_2], \\ R_k(s) = R_o + \mu_k, & s \in C_3 = [s_2, l_c], \\ R_k(s) = +\infty, & s \in S = [l_c, d]. \end{cases}$$

Denoting by $\theta_k^0 = \frac{\mu_k \pi}{R_o}$ the starting angular position, the angle after running s meters is

$$\begin{cases} \theta_k(s) = \theta_k^0 + s/(R_o + \mu_k), & s \in C_1 \\ \theta_k(s) = \phi_o + (s - s_o)/(R_i + \mu_k), & s \in C_2 \\ \theta_k(s) = \pi - (l_c - s)/(R_o + \mu_k), & s \in C_3 \end{cases}$$

Appendix A.4. Clothoid track

Let us study the design of a modified standard track in which the circular part of radius R is bracketed by two smoother junctions of length \bar{l} with continuous curvature. We choose to use a junction whose curvature is linear with respect to the distance, called a clothoid (also known as Euler curve or Cornu spiral). The angle with the tangent φ is

$$\varphi(s) = \frac{sc(s)}{2}$$

where $c(s)$ is the curvature at distance s . Then, since the total angle for the circular part and the two clothoid junctions is π , and using the same notations as before that is l_s is the length of the straight part and l_c the length on the circle, we find

$$\frac{l_c}{R} + 2\varphi(\bar{l}) = \pi.$$

Since the total angle for one clothoid is $2\varphi(\bar{l}) = \bar{l}/R$, this equation leads to $l_c + \bar{l} = R\pi$. Moreover $l_s + l_c + 2\bar{l} = d$ where d is the distance of the race, that is $200m$ in our case, thus $R\pi = d - l_s - \bar{l}$. We find therefore that when there is a junction with a clothoid, the radius of the circular part gets smaller than in the case of a full half circle.

On the clothoid, for $s \in [s_{begin}, s_{end}]$, the expression of the curvature is linear:

$$c(s) = c_{begin} \frac{s_{end} - s}{s_{end} - s_{begin}} + c_{end} \frac{s - s_{begin}}{s_{end} - s_{begin}}.$$

In our case the clothoids will join the straight part (curvature 0) and circular part (curvature $1/R$).

Similarly to the double bend track, we denote by C_1, C_2, C_3, S respectively the first clothoid, circular, second clothoid, and straight parts. We denote by l_s the straight line length, R, l_c the radius and length of the circular part, and $\bar{l}_{1,2}$ the length of the two clothoid junctions. As before, we call $R_k = \frac{l_c + \bar{l}}{\pi} + 1.22(k - 1)$ and $l_{c,k} = l_c(1 + 1.22(k - 1)/R)$ the radius and length of the circular part at lane k . On lane 1, both clothoids have same length \bar{l} , while for $k > 1$ the first clothoid is shorter in order to keep the same total length. The second clothoid has full length $\bar{l}_{k,2} = \bar{l}_k = \bar{l}(1 + 1.22(k - 1)/R)$. Thus the first clothoid has length $\bar{l}_{k,1} = d/2 - l_s - l_c - \bar{l}_{k,2}$.

Taking these variable lengths into account, the curvature at lane k after running s meters is

$$\begin{cases} c_k(s) = \frac{1}{R_k} \frac{s + \bar{l}_k - \bar{l}_{k,1}}{\bar{l}_k}, & s \in C_1 = [0, \bar{l}_{k,1}], \\ c_k(s) = 1/R_k, & s \in C_2 = [\bar{l}_{k,1}, \bar{l}_{k,1} + l_{c,k}], \\ c_k(s) = \frac{1}{R_k} \frac{\bar{l}_{k,1} + l_{c,k} + \bar{l}_{k,2} - s}{\bar{l}_{k,2}}, & s \in C_3 = [\bar{l}_{k,1} + l_{c,k}, \bar{l}_{k,1} + l_{c,k} + \bar{l}_{k,2}], \\ c_k(s) = 0, & s \in S = [\bar{l}_{k,1} + l_{c,k} + \bar{l}_{k,2}, d]. \end{cases}$$

Appendix A.5. Distance gap between two runners

For the interaction term, we need to define the relative distance between the runner on lane 1 and on lane 2, taken by convention at time $y_1(s)$:

$$\rho(s) = x_1(y_1(s)) - x_2(y_1(s)) = s - x_2(y_1(s)).$$

Thus, runner 1 is ahead of runner 2 at time $y_1(s)$ when $\rho(s) > 0$, and behind otherwise. However the term $x_2(y_1(s))$ (of derivative $\dot{x}_2(y_1(s)) = 1/\dot{y}_2(y_2^{-1}(y_1(s)))$) is rather difficult to handle numerically. Therefore, we replace $\rho(s)$ with a more handy approximation of the distance between runners, namely the mean velocity multiplied by the times difference

$$r(s) = (y_2(s) - y_1(s)) \frac{v_1(s) + v_2(s)}{2}.$$

On a curved track, this approximation is adjusted by projecting the two runners on a median circle, while also taking into account the staggered start on different lanes:

$$r(s) = (y_2(s) - y_1(s)) \frac{v_1(s) + v_2(s)}{2} + (\theta_1(s) - \theta_2(s)) \frac{2}{c_1(s) + c_2(s)},$$

where $c_i(s) = 1/R_i(s)$ is the curvature at distance s .

In the indoor case, the first circular part ends at $l_k = R_k(\pi - \theta_k^0)$ which depends on the lane. Therefore, on the first straight part $r(s)$ must also be corrected by the additional term $-(l_{k_1} - l_{k_2})$, where k_1, k_2 are the two lanes.

- [1] IAAF track and field facilities manual. <https://www.iaaf.org/about-iaaf/documents/technical>.
- [2] The physics of running. <https://www.real-world-physics-problems.com/physics-of-running.html>.
- [3] A. Aftalion, L.-H. Despaigne, A. Frenztz, P. Gabet, A. Lajouanie, M.-A. Lorthiois, L. Roquette, and C. Vernet. How to identify the physiological parameters and run the optimal race. *MathS In Action*, 7:1–10, 2016.
- [4] Amandine Aftalion. How to run 100 meters. *SIAM Journal on Applied Mathematics*, 77(4):1320–1334, 2017.
- [5] Amandine Aftalion and Joseph-Frédéric Bonnans. Optimization of running strategies based on anaerobic energy and variations of velocity. *SIAM Journal on Applied Mathematics*, 74(5):1615–1636, 2014.
- [6] R. McNeill Alexander. Stability and manoeuvrability of terrestrial vertebrates. *Integrative and Comparative Biology*, 42(1):158–164, 2002.
- [7] Cécile Appert-Rolland, Hendrik-Jan Hilhorst, and Amandine Aftalion. Nash equilibrium in a stochastic model of two competing athletes. *Journal of Statistical Mechanics: Theory and Experiment*, 2018(5):053401, 2018.

- [8] Horst Behncke. A mathematical model for the force and energetics in competitive running. *Journal of mathematical biology*, 31(8):853–878, 1993.
- [9] A. Boccia and R.B. Vinter. The maximum principle for optimal control problems with time delays. *IFAC-PapersOnLine*, 49(18):951 – 955, 2016. 10th IFAC Symposium on Nonlinear Control Systems NOLCOS 2016.
- [10] F. Bonnans, P. Martinon, D. Giorgi, V. Grelard, S. Maindrault, and O. Tissot. BOCOP - A toolbox for optimal control problems. <http://bocop.org>.
- [11] Debra J Crews. Psychological state and running economy. *Medicine & Science in Sports & Exercise*, 1992.
- [12] Mike D.Quinn. The effect of track geometry on 200- and 400-m sprint running performance. *Journal of Sports Sciences*, 27(1):19–25, 2009.
- [13] L. Gollmann and H. Maurer. Theory and applications of optimal control problems with multiple time-delays. *Journal of Industrial and Management Optimization*, 10(2):413–441, 2014.
- [14] P.R. Greene. Running on flat turns: experiments, theory, and applications. *Journal of biomechanical engineering*, 107(2):96, 1985.
- [15] T. Guinn. Reduction of delayed optimal control problems to nondelayed problems. *Journal of Optimization Theory and Applications*, 18(3):371–377, Mar 1976.
- [16] C. Hanon and C. Thomas. Effects of optimal pacing strategies for 400-, 800-, and 1500-m races on the $\dot{V}O_2$ response. *Journal of sports sciences*, 29(9):905–912, 2011.
- [17] HJ Hilhorst and C Appert-Rolland. Mixed-strategy nash equilibrium for a discontinuous symmetric n-player game. *Journal of Physics A: Mathematical and Theoretical*, 51(9):095001, 2018.
- [18] Wouter Hoogkamer, Shalaya Kipp, Jesse H Frank, Emily M Farina, Geng Luo, and Rodger Kram. A comparison of the energetic cost of running in marathon racing shoes. *Sports Medicine*, 48(4):1009–1019, 2018.
- [19] Joseph B. Keller. Optimal velocity in a race. *American Mathematical Monthly*, pages 474–480, 1974.
- [20] Samuel Lemerancier, Asja Jelic, Richard Kulpa, Jiale Hua, Jérôme Fehrenbach, Pierre Degond, Cécile Appert-Rolland, Stéphane Donikian, and Julien Pettré. Realistic following behaviors for crowd simulation. In *Computer Graphics Forum*, volume 31, pages 489–498. Wiley Online Library, 2012.
- [21] Frank Mathis. The effect of fatigue on running strategies. *SIAM review*, 31(2):306–309, 1989.
- [22] Jean-Benoît Morin, Jean Slawinski, Sylvain Dorel, Antoine Couturier, Pierre Samozino, Matt Brughelli, Giuseppe Rabita, et al. Acceleration capability in elite sprinters and ground impulse: Push more, brake less? *Journal of biomechanics*, 48(12):3149–3154, 2015.
- [23] Hayato Ohnuma, Masanobu Tachi, Akihito Kumano, and Yuichi Hirano. How to maintain maximal straight path running speed on a curved path in sprint events. *Journal of Human Kinetics*, 62(1):23–31, 2018.
- [24] Mike Quinn. The effects of wind and altitude in the 400-m sprint. *Journal of sports sciences*, 22(11-12):1073–1081, 2004.
- [25] Gary J Ryan and Andrew J Harrison. Technical adaptations of competitive sprinters induced by bend running. *New Studies in Athletics*, 18(4):57–70, 2003.
- [26] P. Samozino, G. Rabita, S. Dorel, J. Slawinski, N. Peyrot, E. Saez de Villarreal, and J.-B. Morin. A simple method for measuring power, force, velocity properties, and mechanical effectiveness in sprint running. *Scandinavian Journal of Medicine & Science in Sports*, 26(6):648–658, 2016.
- [27] MJ Stones. Running under conditions of visual input attenuation. *International Journal of Sport Psychology*, 11(3):172–179, 1980.
- [28] James R Usherwood and Alan M Wilson. Accounting for elite indoor 200 m sprint results. *Biology Letters*, 2(1):47–50, 2006.
- [29] William Woodside. The optimal strategy for running a race (a mathematical model for world records from 50 m to 275 km). *Mathematical and computer modelling*, 15(10):1–12, 1991.